Robotics and Computer-Integrated Manufacturing 40 (2016) 34–43

Contents lists available at ScienceDirect

Robotics and Computer-Integrated Manufacturing

journal homepage: www.elsevier.com/locate/rcim

Regular Articles

# A model-based adaptive controller for chatter mitigation and productivity enhancement in CNC milling machines

Carlos Maximiliano Giorgio Bort [a], Marco Leonesio [b,*], Paolo Bosetti [a]

[a] University of Trento, Department of Industrial Engineering, Italy
[b] CNR – Institute of Industrial Technologies and Automation, and Paolo Bosetti, Italy

ARTICLE INFO

*Article history:*
Received 3 July 2015
Received in revised form
7 December 2015
Accepted 20 January 2016

*Keywords:*
Machine tool
Milling
Process control
Optimal Control Theory, chatter

ABSTRACT

Seeking a higher level of automation, according to Intelligent Manufacturing paradigm, an optimal process control for milling process has been developed, aiming at optimizing a multi-objective target function defined in order to mitigate vibration level and surface quality, while preserving production times and decreasing tool wear rate. The control architecture relies on a real-time process model able to capture the most significant phenomena ongoing during the machining, such as cutting forces and tool vibration (both forced and self-excited). For a given tool path and workpiece material, an optimal sequence of feedrate and spindle speed is calculated both for the initial setup of the machining process and for the continuous, in-process adaptation of process parameters to changes the current machining behavior. For the first time in the literature, following a *Model-Predictive-Control* (*MPC*) approach, the controller is able to adapt its actions taking into account process and axes dynamics on the basis of Optimal Control theory. The developed controller has been implemented in a commercial CNC of a 3-axes milling machine manufactured by Alesamonti; the effectiveness of the approach is demonstrated on a real industrial application and the performance enhancement is evaluated and discussed.



## 1. Introduction

In the last 20 years the rapid evolution of products, changing of user needs, and global competition have forced companies to redesign manufacture chains thus taking into account not only the mere productivity, but also the quality, economy, and the flexibility of the production. These reasons motivated an increasing number of enterprises to research and evolve their production systems towards paradigm of *intelligence manufacturing* [1,2]. Increasing of automation in manufacturing systems has both technological and economical impact on a wide sectors of production chains. Optimal control can be exploited to optimize multi-objective target functions defined in order to reduce production times, costs, and increase the quality. The cooperation of multiple intelligent systems will moreover ease the definition and calibration of reliable models of the process [3], thus improving the goodness of the calculated optimal controls. In this scenario, the Computer Numerical Controlled (CNC) machine tools have become popular and have played a key role in workshops, leading to a vast area of research on machining process modeling and optimization [4].

Despite the continuous performance enhancements, since 1968 when the first machining center was marketed, the automation level has not been evolving as much as in other mechatronic fields like robotic vehicles, planes, anthropomorphic manipulators, and humanoids. Advanced robots have perception layers to sense, reconstruct, and learn their state, can plan on line the future actions to take in order to achieve a specified goal. When dealing with machine tools, these features could be aimed at ensuring the operation at optimal cutting conditions, which are constantly identified based on a theoretical knowledge of the process and on the current state of the machine.

Effectiveness and reliability of intelligent systems depend on the level of accuracy of the description of processes. A *good* model captures the most significant phenomena ongoing during the machining, such as force level, material removal rate, tool wear, tool deflection and vibration. The latter is the more critical issue for machine users, since it has effect on the surface quality achieved by the cut, on the stresses acting on the tool and machine components. Vibrations generated during machining can be classified into forced vibrations and self-excited (also called chatter). The former are due to the excitation of the natural frequencies of the tool-workpiece system by the discontinuous cutting forces. In this case the dynamics of the system is stable and tends to be damped. On the other side, self-excited vibrations are mainly due to regenerative effect, namely, a phase shift between vibration

* Corresponding author.
*E-mail address:* marco.leonesio@itia.cnr.it (M. Leonesio).

http://dx.doi.org/10.1016/j.rcim.2016.01.006
0736-5845/

waves left on the inner and outer surfaces of the cut chip. As the cut proceeds, the dynamics of the system becomes unstable, thus increasing progressively the chip thickness and consequently the magnitude of the cutting forces. Such unstable condition reduces the quality of the cut, as well as geometrical accuracy of the generated surfaces, but also might be dangerous for the tool, spindle and machine structure.

The key to predict and control regenerative chatter is the so-called Stability Lobes Diagram (SLD), which shows the boundary between chatter-free machining operations and unstable processes in terms of axial depth of cut as a function of spindle speed: the diagram is characterized by a critical depth of cut, that is the limit under which cutting is stable for all spindle speeds, and by several stability pockets, namely, particular spindle speeds where the stable depth reach higher levels. One of the main contributions to SLD computation in milling was given by Altintas [5], who developed a break-through approach that takes into account a 2DoF dynamics and the average cutting force vector. The main assumption at the core of this model was a linear dependency of the cutting force with respect to the chip thickness and the predominance of the average component in the force spectrum.

Several works have been carried out in the past tackling in-process chatter control in milling operations. Adopting a feedback strategy on any signal correlated to vibrations onset (forces, acceleration, sound, etc.), chatter control can be performed even without computing SLD: the most popular technique belonging to this category is the so-called spindle speed tuning, consisting in regulating the spindle speed on the basis of the measured chatter frequency (see for instance [6] or [7]). This approach is rather profitable, whereas it does not require any characterization of machine dynamics. Another approach involves the exploitation of active [8] or passive [9–11] damping devices, aimed at dissipating the vibrational energy due to instability. One of the first implemented active chatter suppression systems was developed by Dohner et al. [12]. The authors actively generated the lobes stability diagram of the cutting system, thus identifying spindle speeds that ensured a stable process. In this system the spindle was sensed through strain gages at tool root, and it was dumped through a piezo-electric actuator. A further example of active piezo-electric actuators utilized to reduce the dynamic displacement between the tool and workpiece was given by Abele et al. [13]. Moradi et al. [14] proposed a $H_\infty$ control algorithm to control a piezo-electric actuator, used as chatter damper, under tool wear and parameter uncertainties. In a more recent study, Moradi et al. [15] exploited a *Linear Quadratic Regulator* (LQR) to suppress self-regenerative vibrations. This technique allowed the authors to use a non linear model of the process in which forces and chip thickness were related by a cubic relationship. The controls were the counterbalance forces exerted by external actuators, and the target function was defined in order to limit the chatter while minimizing the efforts of the controls. The last effective strategy nowadays being studied to mitigate the chatter is called *spindle speed variation*. It consists in continuously changing the spindle speed with a sinusoidal pattern around the mean speed to disturb the regenerative mechanism. The main advantage of this technique is that it does not require expensive tool holders and it can be implemented on modern CNCs. The calibration of this methodology however can be difficult. Hajikolaei et al. [16] used a genetic algorithm to calibrate the amplitude of the speed modulations such that the input energy to the process was minimized. Albertelli et al. [17] propose a method to optimize sinusoidal spindle speed variation parameters in the simple case of one dominant vibration mode: it is based on the computation and optimization of the phase shift between inner and outer chip modulation assuming a quasi-steady state condition.

Also tool deflection is recognized to provoke detrimental effects both on workpiece geometrical accuracy and surface roughness, as demonstrated by Costes and Moreau in [18]. This fact leaded to the development of specific models able to predict tool deflection in order to compensate and/or limit it by changing cutting parameters (for instance [19]).

The tool wear is another crucial performance affecting machining efficiency and it should be estimated as accurately as possible and permanently kept under control [20]. As a matter of fact, the tool wear has a large influence on the economics of machining operation: in fact, it affects not only the tool life but also the quality of the final product in terms of residual stress and surface integrity. Even in this case, several models have been developed in order to predict tool wear, above all when dealing with hard materials [21], often aimed at optimizing process parameters to increase tool life. While milling process modeling is often used for the off-line optimization of the part program [22], no works can be found merging such a pre-processing phase with axes dynamics in order to exploit properly the *a priori knowledge* about cutting process and machine responsiveness. Moving from these considerations, this paper presents the first system for fast optimization of process parameters for milling operations markedly spindle rotational speed and tool feedrate based on *Optimal Control Theory*. A suitable target function is defined on the basis of a model of the machine tool dynamics and the cutting process: it is specifically designed to suppress/mitigate vibration occurrence, while taking into account tool wear, tool deflection and productivity (material removal rate). Then, an optimal sequence of controls for a given path and workpiece material can be calculated both for the initial setup of the machining process and for the continuous, in-process adaptation of process parameters to changes in process behavior. The model capabilities include the prediction of self-excited and forced vibration (which is the main objective), tool wear, tool deflection, spindle force and power, feed axes response by means of a simplified first order dynamics. The developed controller has been implemented in a commercial 3 axes boring machine manufactured by Alesamonti. Machine dynamics, necessary for feeding the process model, has been measured via tap testing in several tool positions over the allowable work volume and, then, interpolated in order to get the dynamic response in every position along the tool path. The process model exploits commercial CSG (Constructive Solid Geometry) libraries, that provide methods and structures for tool-workpiece intersection, allowing the computation of MRR, depth of cut and engagements arcs that are needed by cutting force model. Once the various performance parameters are weighted in a single objective function, an advanced optimization engine is exploited for determining the proper control action. The paper is structured as follows: in Section 2 the controller architecture is framed together with a detailed description of the components of the objective function. In Section 3, the dynamic characterization of the test machine is presented and the results validated by means of stable and unstable milling passes. In Section 4 the controller effectiveness is demonstrated on the test machine for a real industrial application: the performance enhancement due to the introduction of the proposed innovative controller is discussed. In Section 5 the conclusions are reported.

## 2. Adaptive controls for CNC machines

Adaptive controllers (ANC) are devices that regulate process parameters to achieve a certain performance. In the case of milling process, the controls on which ANC acts are the spindle speed and the feed rate. A recent review of ANC system was given by Stavropoulos et al. [23]. Ulsoy and Koren [24] identified three types of ANC:

1. *Adaptive Control with Constraints (ACC)* typically are aimed at maximizing the cutting force within the limits imposed by the maximum stress that the tool can tolerate without breakage.
2. *Geometry Adaptive Control (GAC)* are used in finishing cuts, where the main objective is to achieve a high-quality surface, which can be described by a high geometrical accuracy, good surface integrity, as well as low roughness.
3. *Adaptive Control with Optimization (ACO)* in which the process parameters are computed and regulated in order to optimize a certain index or performance, such as reduction of vibration, increasing of productivity, improvement of surface quality, and control of the tool wear.

The controller developed in this study belongs to the third category. The purpose is to propose a novel approach to enhance adaptive systems by including a reliable adaptive model describing cutting conditions: the adaptive controller exploits the model to allow stable cuts (free of forced and self-excited vibrations), a reduced tool wear and tool deflection, while preserving productivity and satisfying the constraints related to spindle power and torque.

### 2.1. Optimal control

The *optimal control* (OC) is a technique to control a dynamic system by calculating a set of controls which minimize a desired performance, while ensuring that the found solution is the best among all the admissible ones. OC has become very popular in the last years thanks to the improvement of performances of modern computers, thus allowing the solution of complex systems of differential and algebraic equations (DAE) in real-time [25]. For CNC machines the target function to be optimized can be defined by the weighted sum of terms associated to process productivity, quality, and costs.

The Bolza optimal control problem [26] formulated in this study represents a step foreword of the work done by Bosetti et al. [27]. The target function is defined by the weighted sum of four terms, plus the Mayer contribute used to avoid that the computed feed rate is too different from the nominal one:

$$\begin{cases} \min\limits_{u(\zeta)} & J(u(\zeta),x(\zeta)) = w_i\left(\dfrac{f(\zeta_i)-f_i}{f_{min}}\right)^2 + \displaystyle\int_{\zeta_i}^{Z} w_{MRR}\,F_{MRR}(u(\zeta),x(\zeta)) \\ & \qquad + w_{Ra}\,F_{Ra}(u(\zeta),x(\zeta)) + w_w\,F_w(u(\zeta),x(\zeta)) \\ & \qquad + w_{en}\,F_{en}(u(\zeta),x(\zeta)) \\ & \qquad + w_{forced}\,F_{forced}(u(\zeta),x(\zeta)) \\ & \qquad + w_{chatter}\,F_{chatter}(u(\zeta),x(\zeta))\,d\zeta \\ \text{s. t.} & \\ & f(\dot{x}(\zeta),x(\zeta),u(\zeta)) = 0 \quad \text{Dynamics of the system} \\ & (x(\zeta),u(\zeta)) \in C(x(\zeta),u(\zeta)) \quad \text{Path constraints} \\ & B(x(Z)) = 0 \quad \text{Boundary conditions} \\ & x(0) = \hat{x} \quad \text{Initial conditions} \end{cases} \tag{1}$$

where the independent variable $\zeta$ is the curvilinear abscissa of the mill; $x(\zeta)$ is the state of the machine represented by the actual feed rate and spindle speed; $u(\zeta)$ is the control command vector, whose elements are the magnitude of the axes acceleration $\dot{f}(\zeta)$, and spindle angular acceleration $\dot{\omega}(\zeta)$. Process productivity is maximized by the term $F_{MRR}(u(\zeta),x(\zeta))$ which is the instantaneous MRR. The costs of the process are taken into account by the terms $F_w(u(\zeta),x(\zeta))$ and $F_{en}(u(\zeta),x(\zeta)) + w_{forced}$ associated to the tool wear and energy spent during the cut, respectively. Finally, the quality of the process is maximized by including three terms considering the roughness of the cut surfaces $F_{Ra}(u(\zeta),x(\zeta))$ (which is considered affected by the average level of cutting force, as explained in [27]), forced vibrations $F_{forced}(u(\zeta)$, and chatter $F_{chatter}(u(\zeta)$ (see Section 2.2.3). As a matter of fact, even if also vibrations obviously affect surface roughness, these latter components also produce tool and spindle damages/wear.

To ensure the feasibility of the OCP solution, constraints are imposed on the machine performance (maximum spindle speed, feed rate, cutting torque and power):

$$(x(\zeta),u(\zeta)) \in C(x(\zeta),u(\zeta)) = \begin{cases} \omega_{min} \le \omega(\zeta) \le \omega_{max} \\ f_{min} \le f(\zeta) \le f_{max} \\ Tc(\zeta) \le Tc_{max} \\ Pc(\zeta) \le Pc_{max} \\ f(\zeta) \le \dfrac{0.6}{2\pi}\,rf\;\omega(\zeta)\,on\_off\left(10^6\,crossSection(\zeta)\right) \end{cases} \tag{2}$$

The last path constraint is suggested by tool manufacturer and expert CNC users: it is aimed at preserving tool integrity. *on_off* () function is responsible to activate this constraint only in the tool path segments along which the mill is cutting; *crossSection*$(\zeta)$ is given by the process simulator and returned the instantaneous cut cross section.

The dynamics of the axes are described by as a first order system, thus taking into account the filtering effect of their inertia:

$$f(\dot{x}(\zeta),x(\zeta),u(\zeta)) = \begin{bmatrix} f(\zeta)\dfrac{d}{d\zeta}f(\zeta) - vf(\zeta) \\ f(\zeta)\dfrac{d}{d\zeta}\omega(\zeta) - v\omega(\zeta) \end{bmatrix} = \begin{bmatrix} 0 \\ 0 \end{bmatrix} \tag{3}$$

### 2.2. Mitigation of vibrations

Material removal processes produce two main types of vibrations: self-excited vibrations and forced vibrations [28]. Forced vibrations appear due to the direct excitation of natural modes of the machine by the discontinuous cutting edge engagement. In this case, vibrations can be limited decreasing cutting force level and/or shifting its harmonic components by varying spindle speed. Anyway, such a kind of vibrations rarely represents a problem in the common machining practice.

Self-excited vibrations due to regeneration mechanism (*regenerative chatter*, or simply *chatter*) are a form of dynamic instability. When the cutting force creates a relative displacement between flexible tool and workpiece at the cutting point, the chip thickness experiences waves on its inner and outer surfaces due to present and past vibrations. Depending on the gain of the system and the phase between the inner and outer waves, the dynamics of the cutting system can be unstable, leading to exponentially growing chips, hence large forces and vibrations until the tool jumps out of the cut or machine tool setup is damaged. In this work, tool vibration analysis is twofold, as it treats both chatter and forced vibrations. In order to avoid and control chatter occurrence, the off-line optimization phase is enhanced with a stability analysis based on regenerative chatter theory along the curvilinear abscissa, while a heuristic approach is exploited to estimate the forced vibration level: the analysis is fed by the cross section characteristics coming from G-code processing and by the dynamic compliance matrix at tool tip (that is assumed to be measured).

#### 2.2.1. Stability analysis

Chatter occurrence is influenced by several factors that can be grouped into two main categories: process factors (material, tool geometry, lubrication, etc.) and dynamic factors (tool-workpiece relative dynamic compliance). The relationship between stability occurrence and the above-mentioned factors can be analyzed through a reduced set of variables by means of two main approaches: the multi-frequency and the single-frequency 0-order approach (*ZOA*). The single-frequency model allows a fast and accurate stability lobe calculation for non-interrupted milling processes. Due to the fact that cutting stability heavy-duty milling

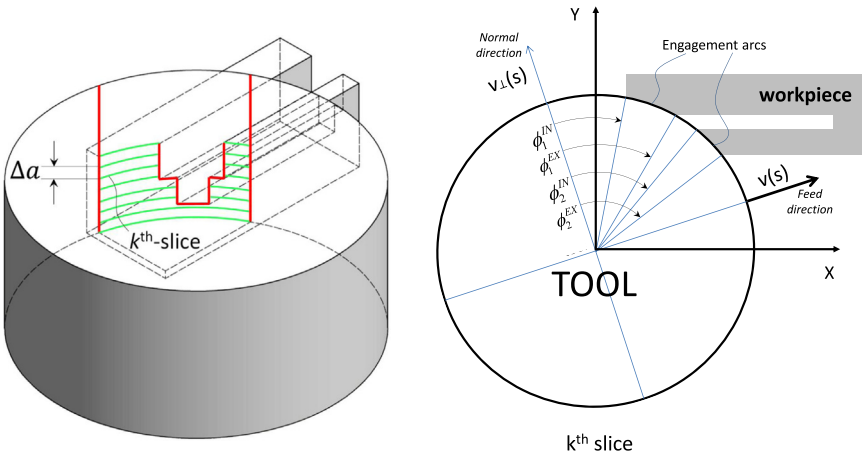


**Fig. 1.** Engagement arcs definition w.r.t. feed velocity.

operations are usually performed with large (75÷80%) tool engagements and high number of flutes, the created harmonics are usually weak, and the single-frequency method can provide an accurate solution [29]. Adopting this latter approach, stability analysis is traced back to the following characteristic equation of the dynamic system machine tool+milling process:

$$\det\left(\mathbf{I} + \Lambda\mathbf{A}_0\left(\zeta\right)\hat{\mathbf{G}}_{tool-wp}\left(s|\zeta\right)\right) = 0 \tag{4}$$

with

$$\Lambda = -\frac{N_{cut}}{4\pi}bK_t\left(1 - e^{-(\sigma+i\omega)2\pi/\Omega N_{cut}}\right) \tag{5}$$

where $\mathbf{A}_0$ is a matrix that takes into account the orientation of the average cutting force w.r.t. feed and normal axes, and depends on tool engagement condition together with tangential and radial cutting pressures (hereafter $K_t$ and $K_r$, respectively); $\hat{\mathbf{G}}_{tool-wp}$ is the relative dynamic compliance between tool and workpiece in the complex variable $s = \sigma + j\omega$, defined w.r.t. the same reference frame of $\mathbf{A}_0$ (without loss of generality, since in our application the workpiece is extremely rigid, only the tool compliance is taken into consideration, namely, $\hat{\mathbf{G}}_{tool-wp} \simeq \hat{\mathbf{G}}_{tool}$); $b$ is the depth of cut; $N_{cut}$ is the number of tool cutters; $(\sigma + i\omega)$ is the pole of the dynamical system and $\Omega$ is the spindle speed in rad/s.

Imposing $\sigma = 0$ and scanning the chatter frequency $\omega$, (5) can be used to map the stability limit w.r.t. depth of cut and spindle speed (the result is the well-known SLD). On the other side, given depth of cut and spindle speed, (4) and (5) could be solved w.r.t. $\sigma$ and $\omega$, where $\sigma$ in particular expresses the exponential growth of vibration during unstable cut and could be used as a metric to measure the instability/stability level. Unfortunately, this latter equation system is transcendent and the solution could be found only through time-consuming numerical algorithms. A viable heuristic solution consists in computing the stability limit and, then, evaluating the instability level by the difference between the actual depth of cut and the limiting one. In this sense, the SLD itself is used to generate a penalty function relating instability level to spindle speed.

In (4), compliance matrix $\hat{\mathbf{G}}_{tool}$ depends on curvilinear abscissa not only in terms of tool position along the tool path, but also in terms of feed velocity direction. The dependence of $\hat{\mathbf{G}}_{tool}$ on feed velocity unitary vector ($\mathbf{v}$) can be expressed by applying a rotation to the dynamic compliance measured w.r.t. the global machine axes:

$$\hat{\mathbf{G}}_{tool}(\zeta|\omega) = \mathbf{R}(\mathbf{v})\mathbf{G}^{axes}_{tool}(\zeta|\omega) \tag{6}$$

with

$$\mathbf{R}(\mathbf{v}) = \begin{bmatrix} v_x & -v_y \\ v_y & v_x \end{bmatrix} \tag{7}$$

The dynamic compliance at tool tip must be measured, or estimated, for a given tool and for a suitable number of position samples along the tool path, wherever SLDs have to be computed. Since the measurement of the necessary set of dynamic compliances may be quite onerous, a viable makeshift consists in interpolating an adequate mesh of primitive dynamic compliances covering the available workspace (as explained in Section 3.1). On the other side, the response at tool tip can be derived from that at spindle nose by exploiting the well-known receptance coupling sub-structuring technique [30]: in this way the measurements do not have to be repeated whenever the tool is changed.

The orientation matrix $\mathbf{A}_0$ relates the vibrational displacement of the tool along feed and normal direction to the average cutting force vector due to the consequent material removal. The matrix can be computed integrating w.r.t. the angular position the forces exerted by each cutter engaged in the workpiece; thus, tool engagement condition raises to a key role in modeling the process. In particular, considering the cylinder bounding the cutters, tool engagement can be described by the arcs of contact between this cylinder and the workpiece. In the general case concerned with any possible tool path and workpiece, the arcs of contact may be more than one for each tool section and vary along the tool axis (see Fig. 1). In order to deal with such inherent complexity, the list of the contact arcs for each tool slice is computed by a dedicated code that exploits commercial 3D CSG libraries (*ACIS*, developed by *Spatial*® Corporation). Once the tool engagement is properly described, matrix $\mathbf{A}_0$ can be computed as it follows (i.e., the generalization of the corresponding quantity presented in [5]):

$$\mathbf{A}_0 = \begin{bmatrix} a_{ff} & a_{fn} \\ a_{nf} & a_{nn} \end{bmatrix} \quad \text{with}$$

$$a_{ff} = \frac{1}{a_{tot}}\sum_k \Delta a \sum_i \frac{1}{2}(\cos 2\phi - 2K_r\phi + K_r \sin 2\phi)\Big|_{\phi^{IN}_{k_i}}^{\phi^{EX}_{k_i}}$$

$$a_{fn} = \frac{1}{a_{tot}}\sum_k \Delta a \sum_i \frac{1}{2}(-\sin 2\phi - 2\phi + K_r \cos 2\phi)\Big|_{\phi^{IN}_{k_i}}^{\phi^{EX}_{k_i}}$$

$$a_{nf} = \frac{1}{a_{tot}}\sum_k \Delta a \sum_i \frac{1}{2}(-\sin 2\phi + 2\phi + K_r \cos 2\phi)\Big|_{\phi^{IN}_{k_i}}^{\phi^{EX}_{k_i}}$$

$$a_{nn} = \frac{1}{a_{tot}}\sum_k \Delta a \sum_i \frac{1}{2}(-\cos 2\phi - 2K_r\phi - K_r \sin 2\phi)\Big|_{\phi^{IN}_{k_i}}^{\phi^{EX}_{k_i}} \tag{8}$$

where $a_{tot}$ is the total tool depth engaged in the workpiece, $\Delta a$ is

the tool discretization spacing is axial direction, $\phi_{k_i}^{IN}$ and $\phi_{k_i}^{EX}$ are, respectively, the initial and the exit angle of the $i$th arc of the $k$th tool slice. It is worth to be remarked that ZOA approach assumes that $\mathbf{A}_0$ and $\hat{\mathbf{G}}_{tool}(\omega|\zeta)$ do not depend on time, while, as matter of fact, this assumption does not hold in the case of complex tool trajectories born by a general part program, since tool engagement varies continuously as well as structural machine dynamics. However, the assumption can be considered still valid on the basis of the so-called frozen time approach based on the "Adiabatic Theorem", also adopted to tackle variable time delay systems [31]. It states: *A physical system remains in its instantaneous eigenstate if a given perturbation is acting on it slowly enough and if there is a gap between the eigenvalue and the rest of the system spectrum* [32].

Declining the theorem in the case under consideration, since in the ZOA approach a single eigenvalue (or pole) is considered to be relevant, adiabatic condition is assured by the sole perturbation slowness. In practice, if in a time window $\Delta T$ the variation of the product $\mathbf{A}_0\hat{\mathbf{G}}_{tool}$ is negligible and $\Delta T$ is much greater than the tooth passing period, the system dynamics (whose pole is given by $(\sigma + i\omega)/\tau$) is much more faster than the perturbation action and the time-varying $\mathbf{A}_0\hat{\mathbf{G}}_{tool}$ can be assumed to be frozen in the interval $\Delta T$, i.e.,

$$\mathbf{A}_0\hat{\mathbf{G}}_{tool}\big(\zeta(t)\big) \approx \text{const.} \quad \text{for} \quad t \in \Delta T \tag{9}$$

Since the chatter frequency is a function of spindle speed, the variability of $\hat{\mathbf{G}}_{tool}$ must be evaluated for a suitable range of frequency, namely, in the neighborhood of the resonances that are candidate to be source of chatter problems. Algorithmically, the following expression is proposed to verify the consistency of the frozen time assumption:

$$\frac{\| \mathbf{A}_0\Big(\zeta(t_{k+1})\Big)\hat{\mathbf{G}}_{tool}\Big(\omega, \zeta(t_{k+1})\Big) - \mathbf{A}_0\Big(\zeta(t_k)\Big)\hat{\mathbf{G}}_{tool}\Big(\omega, \zeta(t_k)\Big)\|}{\| \mathbf{A}_0\Big(\zeta(t_k)\Big)\hat{\mathbf{G}}_{tool}\Big(\omega, \zeta(t_k)\Big)\|} < \epsilon, \quad \forall\, \omega \in F_c \quad \text{and} \quad t_{k+1} - t_k > M\tau_{TPF} \tag{10}$$

where $\zeta(t_k)$ and $\zeta(t_{k+1})$ are two subsequent curvilinear abscissas, $\tau_{tpf}$ is the tool passing frequency, $\epsilon$ and $M$ two parameters to be set after proper experiments and $F_c$ is the union of neighborhoods of the relevant tool tip resonances. In case (10) is not verified, the stability analysis is unreliable and the corresponding term in the global objective function must be neglected.

The last issue to be tackled concerns the density of the stability analysis that must be performed along the curvilinear abscissa during the process simulation. Indeed, in order to increase the computational efficiency, the SLDs should be updated and stored only if necessary. As in (4) only the eigenvalue $\Lambda$ varies along the tool path (due to changes in tool engagements and dynamics), this quantity itself can be used to drive the SLDs evaluation density. A possible criterion consists in tracking the eigenvalues evolution along the tool path in a range of chatter frequencies; then, SLD is re-calculated and stored only when this difference is greater than a given threshold. Mathematically:

$$\frac{1}{N}\sum_i |\Lambda_k(\omega_i) - \Lambda_{k+j}(\omega_i)| > \epsilon \quad \text{with} \quad \omega_i \in \{\omega_1, \omega_2, \ldots, \omega_N\} \tag{11}$$

where $k$ refers to the last abscissa sample corresponding to a new SLD, $j$ is the sample lapse till the current abscissa, $\omega_i$ are the chatter frequency samples spanning the interval of interest and $\epsilon$ is a parameter to be set on the basis of a trade-off between precision and computational power. Finally, SLDs are used only in a spindle speed range which is feasible from a technological point of view.

### 2.2.2. Forced vibrations

In spite of process stability, even forced vibrations could be significant and detrimental, so they must be considered in the optimization objective as well. Forced vibration level is evaluated by considering the response of the tool tip to the dynamic components of cutting force, that can be computed from tool engagement and cutting parameters (in a similar way than the average component, as explained in [33]).

Starting from the ideal cutting mechanics, the dynamic cutting force components in frequency domain are harmonics of the tool passing frequency. The $r$th harmonic can be written as follows:

$$\mathbf{f}_{dyn}^{(r)}(\zeta) = \frac{1}{4\pi}K_t\frac{a_{tot}}{N(\zeta)}f(\zeta)\begin{Bmatrix} a_{ff}^{(r)} \\ a_{nf}^{(r)} \end{Bmatrix} \tag{12}$$

with

$$\begin{aligned} a_{ff}^{(r)} &= \frac{1}{a_{tot}}\sum_k \Delta a \sum_i \frac{j}{2}\Big( - c_0K_r e^{-jrN_{cut}\phi} + c_1 e^{-jp_1\phi} - c_2 e^{jp_2\phi}\Big)\Big|_{\phi_{k_i}^{IN}}^{\phi_{k_i}^{EX}} \\ a_{nf}^{(r)} &= \frac{1}{a_{tot}}\sum_k \Delta a \sum_i \frac{1}{2}\Big( c_0 e^{-jrN_{cut}\phi} + c_1 e^{-jp_1\phi} + c_2 e^{jp_2\phi}\Big)\Big|_{\phi_{k_i}^{IN}}^{\phi_{k_i}^{EX}} \end{aligned} \tag{13}$$

where $p_1 = 2 + rN_{cut}$, $p_2 = 2 - rN_{cut}$, $c_0 = \frac{2}{rN_{cut}}$, $c_1 = \frac{K_r - j}{p_1}$ and $c_2 = \frac{K_r + j}{p_2}$, with $j$ denoting the imaginary unit (the other symbols have been defined after (8)). The number of relevant harmonics ($r$) of the tooth passing frequency ($\omega_{tpf}$) to be considered for an accurate reconstruction of the dynamic cutting force components depends on the immersion conditions and on the number of teeth in the cut.

Finally, the vibration index can be identified with the magnitude of the resulting tool tip vibrational displacement:

$$F_{forced} = \| \sum_{r\in([-R,R]-\{0\})} \hat{\mathbf{G}}_{tool}(r\omega_{TPF}|\zeta)\cdot\mathbf{f}_{dyn}^{(r)} \| \tag{14}$$

where $R$ is the number of harmonics to be considered (usually 3–5).

### 2.2.3. Spindle speed tuning

When solving the OCP, the optimal spindle speed was given by the linear combination of the terms of the target function associated to surface roughness, tool wear, forced vibration, and chatter. The first three terms were convex with respect to the spindle speed, while multiple optimal solutions were given by the latter. Due to the periodic nature of the stability lobes diagram different values of spindle speed allowed to obtain stable cuts. This fact was taken into account by dynamically formulating $F_{chatter}(u(\zeta))$ according to the instantaneous cutting conditions.

The stability lobes diagram was computed for each position of the tool, Fig. 2. To complete this task the engagement of the mill along the tool path was pre-calculated through the 3D geometric modeling kernel *ACIS* developed by Spatial Corporation. Once the lobes diagram was known, three conditions were identified to formulate $F_{chatter}(u(\zeta))$, based on the actual cutting depth $d(\zeta_k)$, stability limit $d_{lim}$, and position of the highest peak $d_{max}$:

- $d(\zeta_k) \le d_{lim}$: $F_{chatter}(u(\zeta))$ was set equal to zero since all the spindle speed allowed a stable cut.
- $d(\zeta_k) \ge d_{max}$: it was not possible to achieve a stable cut, but in order to limit unavoidable chatter $F_{chatter}(u(\zeta))$ was formulated as a cubic spline with the minimum at the spindle speed corresponding to $d_{max}$.
- $d_{lim} \le d(\zeta_k) \le d_{max}$: the abscissa coordinate of the stability pockets was identified and used to generate a set of nodes that were interpolated with a Piecewise Cubic Hermite Polynomial [34]. Stability pockets close to $d(\zeta_k)$ less than 0.2 mm were

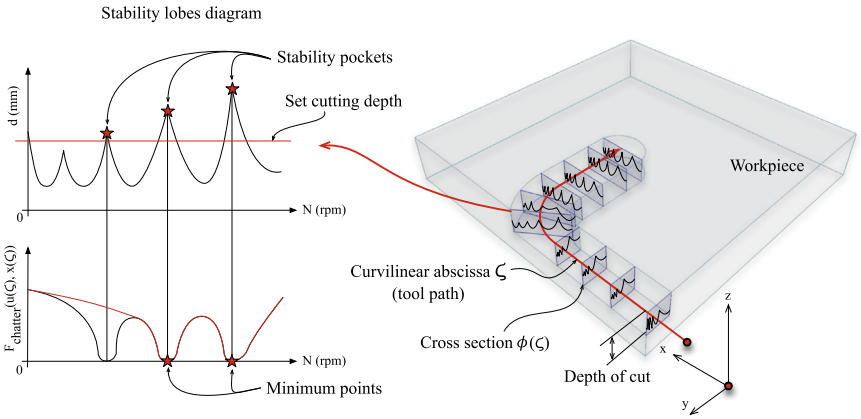


**Fig. 2.** Discretization of the tool path (right) and computation of the target function at each quantized position increment (left).

neglected thus taking into account the uncertainty of the parameters used to compute the stability lobes diagram. To place the minimal points, auxiliary nodes with non-null ordinate were placed between the stable spindle speeds, and the slope at each node was set to zero, Fig. 2.

## 3. System characterization

### 3.1. Dynamic compliance

When calculating lobes stability diagrams, it is important to use a FRF which catches the main modes of the system. The stability lobes diagram is indeed given not only by the stability pockets generated by each mode, but its final shape depends also on the intersection of lobes associated to different modes. If a mode is missing in the FRFs, then the lobes diagram will appear distorted or will not describe the true stability space at all. To identify the dynamic compliance of the machine the system has to be described as a Multiple Input Multiple Output (MIMO), where the inputs were the impacts of the tool on the workpiece along the directions perpendicular to the axis of the mill (i.e., *X* and *Y*), and the outputs are the displacement along these directions. The FRF of such system can be represented by a $2 \times 2$ matrix:

$$FRF = \begin{bmatrix} FRF_{x,x} & FRF_{y,x} \\ FRF_{x,y} & FRF_{y,y} \end{bmatrix} \tag{15}$$

The notation used in this paper is the following: the first subscript indicates the direction along which the impulse was given, while the second subscript is used to specify the direction along which the displacement was measured.

In this study impact tests were performed to measure the four terms of the co-located *FRF* matrix. The ram of the machine was excited through a *PCB 086D20* hammer with a 084A63 hard plastic tip. A three-axial *PCB T356A15* accelerometer was mounted on the tool tip and it was acquired at 2000 Hz, Fig. 3.

An example of calculated FRF is reported in Fig. 4.

The homogeneity of dynamic properties of the machine across the working volume was verified by changing and combining the positions of linear axes according to a design matrix [35]. It was observed that the compliance of the machine did not depend on the positions of the *X*-, *Y*-, and *Z*-axes. Only the position of the ram (i.e., *W*-axis) affected the frequency response of the system. In Fig. 5 are reported, for four positions of the ram, the real and imaginary part of the measured direct FRFs. When the ram was retracted ($W=0$ mm) the first mode was around 850 Hz and not dominant. In this case the system could be considered stiff. On contrary, when the ram was fully extended ($W=-300$ mm) the first mode was dominant and at a lower frequency, approximately 200 Hz.

In order to take into account the ram position-dependent machine stiffness, it was decided to measure the FRFs by changing *W* with an increment of 5 mm. The data were stored into a look-up table, ready to be accessed when the position of the ram was changed. Since the FRFs were discretized along *W*, at intermediate coordinates the data used to compute the lobes diagram were those collected at the closest discretized position.

### 3.2. Stability lobes diagrams

The stability lobes diagram was calculated for the most compliant configurations, that according to Fig. 5 is the one in which the ram is extracted for 300 mm. The procedure followed to obtain the stability lobes diagrams is the one described by Altintas in [36] (see Section 2.2.1).

The stability lobes diagrams was validated by recording the vibrations of the milling machine with a triaxial accelerometer *Dytran*3213*M*6 that was acquired at 10 kHz and was screwed to the cutting head, see Fig. 6. Several face milling cuts of *AA6082-T6* were performed, in order to identify the stability pocket according to the procedure proposed by Bediaga et al. [37]. With this approach, the boundary of the stability lobes diagrams is searched by iteratively adjusting the cutting depth and spindle speed. The chatter onset is quantified by calculating the *energy ratio chatter indicator* ($CI_{ER}$), as proposed by Kuljanic et al. [38]:

$$CI_{ER} = \frac{E_c}{E} = 1 - \frac{E_p + E_n}{E} \tag{16}$$

where $CI_{ER}$ is given by integral quantities related to the Power

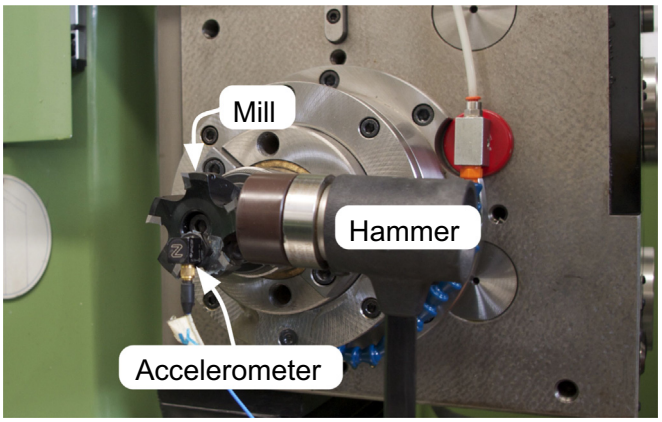


**Fig. 3.** Setup of impact tests.

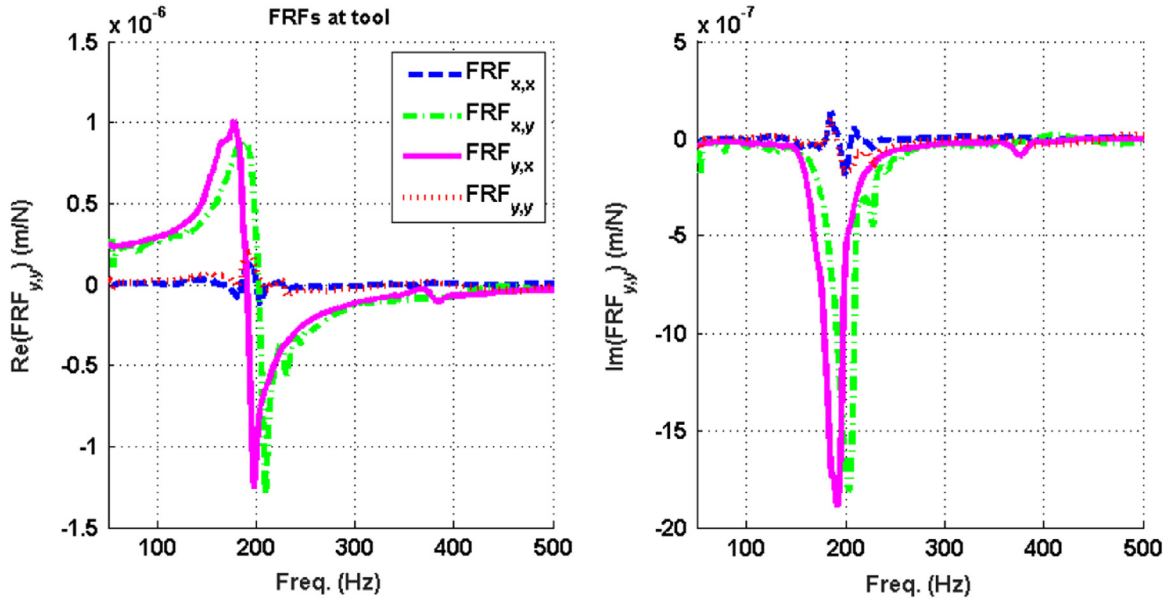


**Fig. 4.** Real part (left) and imaginary part (right) of the FRF measured along directions perpendicular to the spindle. The ram was fully extended ($W$=-300 mm).

Spectrum Density (PSD) of recorded accelerations ($E$), asynchronous component of the signal related to the chatter ($E_c$), synchronous components associated to the forced vibrations ($E_p$), and noise ($E_n$).

High $CI_{ER}$ are given by unstable cuts. Chatter indeed is associated to phase shift of half-period between the vibration of the tool and the tool pass frequency. When this phase shift occurs, the integral of the PSD of $E_p$ becomes smaller, while the integral of the PSD of $E_c$ increases.

Each point in the stability lobes diagram of Fig. 6 has a color and a dimension that is proportional to the calculated $CI_{ER}$; the bigger and more red the point is, the more severe the chatter is. The amplitude of the predicted stability pockets is in agreement with the measurements, but they are slightly shifted to smaller spindle speed. This probably corresponds to a small shift of the limiting resonance, whereas system dynamics during cutting are usually slightly different from those holding during measurement. Nonetheless, for the application proposed in this study the measured stability limits are in agreement with the theoretical calculations.

### 3.3. Cutting force constants

In this study the reference material of the workpiece was *AA 6082-T6*. To compute the lobes diagram it was necessary to estimate the cutting constants of the material through experimental tests. It followed the procedure developed by Altintas [36]. Full-immersion face milling (i.e., slotting) cuts were carried at different feed rates. The used tool, inserts, and spindle speed are listed in Table 1.

Cutting forces parallel and perpendicular to the feed direction ( $\bar{F}_x$ and $\bar{F}_y$, respectively) were measured with a dynamometric

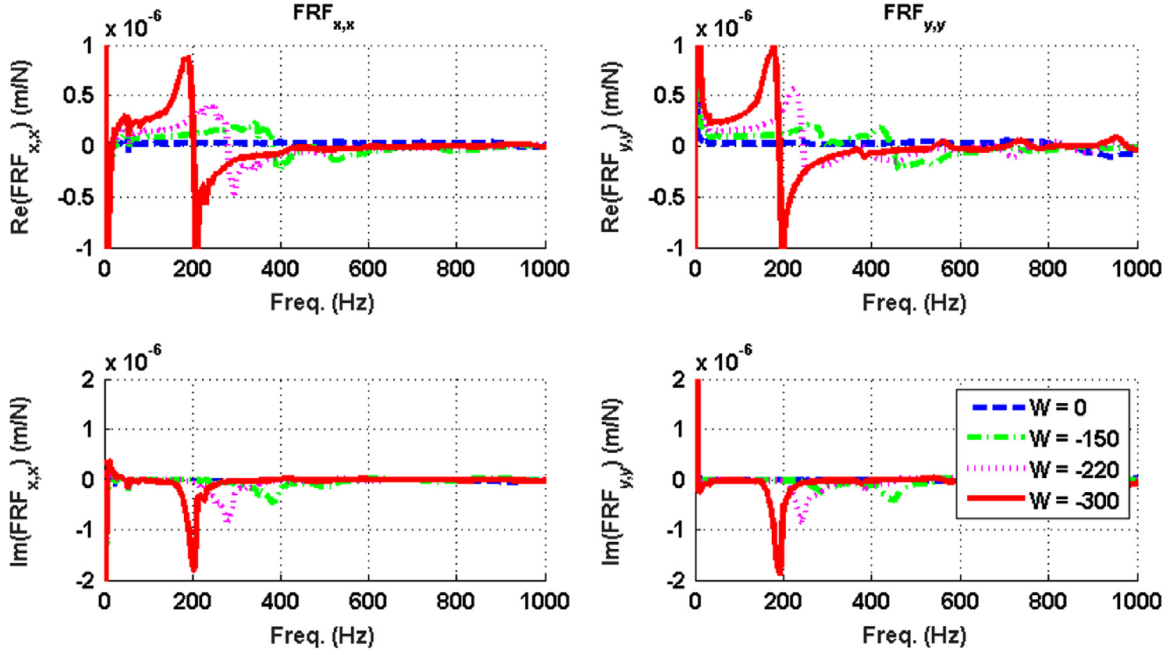


**Fig. 5.** Real and imaginary part of direct FRF along $X$ (top left and bottom left), and real and imaginary part of direct FRF along $Y$ (top right and bottom right).

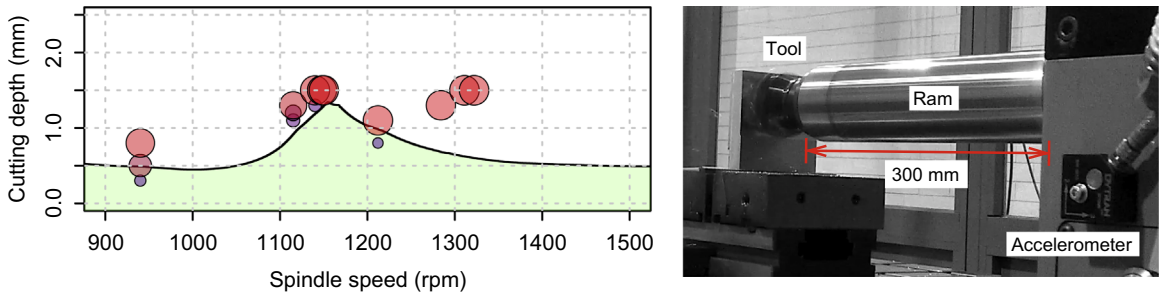


**Fig. 6.** Stability lobes diagram (left), and set-up of measurements for its validation (right). (For interpretation of the references to color in this figure caption, the reader is referred to the web version of this paper.)

**Table 1**
Process parameters used for the cutting force constants identification.

| Parameter | Value |
|---|---|
| Material of the workpiece | AA 6082-T6 |
| Diameter of the mill | 63 mm |
| Number of flutes | 5 |
| Insert | WIDIA XPHT160408-AL |
| Coating of the inserts | TiN |
| Spindle speed | 1500 rpm |
| Depth of cut | 2 mm |
| Width of cut | 63 mm |

table. The measurement system consisted of three 3-component force link *Kistler 9347C* connected to a charge amplifier *Kistler 5073A311*, which were acquired by a *NI cRIO 9012* though a *NI 9215* module. Average cutting forces at each feed rate are reported in Fig. 7. The relationship between cutting forces and chip geometry is assumed to be linear [39], and defined as:

$$\begin{cases} \bar{F}_x = -\dfrac{N\,d}{4} K_{rc} f - \dfrac{N\,d}{4} K_r e \\ \bar{F}_y = +\dfrac{N\,d}{4} K_{tc} f + \dfrac{N\,d}{4} K_t e \\ \bar{F}_z = +\dfrac{N\,d}{4} K_{ac} f + \dfrac{N\,d}{4} K_a e \end{cases} \tag{17}$$

where $f$ is the feed rate, $N$ is the number of flutes in the mill, and $d$ is the cutting depth. $K_{rc}$, $K_{tc}$, and $K_{ac}$ are the cutting constants due to the shear stresses in radial, tangential, and axial directions, respectively, while $K_{re}$, $K_{te}$, and $K_{ae}$ are due to the frictions between the edge of the tool and the workpiece. The values of the coefficients have been identified via Least Squares method and reported in Table 2. The axial component of the cutting force, that is $F_z$, was small and it was almost constant with respect to feed rate. Therefore $K_{ac}$ was considered to be 0 N mm$^2$. Such assumption did not affect the calculation of the lobes diagram, since the model used in this study only considered the forces and vibrations perpendicular to the axis of the spindle.

## 4. Results

The effectiveness of the process controller (from now indicated as *Evaluation Perception Controller* (EPC)), with particular attention to the stability of the process, was tested by performing cuts on a 3-axes industrial milling machine. The reference process was the full-immersion face milling of a *AA6082-T6*, see Table 1. The cutting depth was fixed to 1 mm. Three different cutting conditions were considered: a nominal case in which the process parameters were set according to the suggestions reported in the tool catalog by the tool manufacturer (that is a feed rate of 1000 mm min and a spindle speed of 1500 rpm), a cut in which the EPC was active but the term of the target function associated to the chatter mitigation was deactivated, and the last case in which the chatter mitigation scheme was included in the solution of the optimal control.

The history of controls utilized in the three tests are shown in Fig. 8. A light dotted line indicates the maximum feed rate and spindle speed allowed by the machine. The black dotted line called *nominal* is used for the cuts performed with the parameters suggested by the tool catalogs, and where the feed rate and spindle speed are kept constant across the tool path. The dashed black line *EPC* indicates the controls obtained by solving the optimal control in which the term of the target function associated to the chatter mitigation was deactivated. For this configuration of the EPC, the feed rate is maximum when the mill is not cutting, but when the tool is in contact with the workpiece (i.e., the cross section is different from zero) the feed rate is reduced and the spindle speed is increased to its maximum value, thus ensuring low cutting torques and a good quality of the cut. Finally, the dashed black line *EPC+C.M.* is used to represent the controls obtained by solving the optimal control with the chatter mitigation scheme activated. In this case during the cut the EPC reduces the spindle speed to 1226 rpm that is a value for which the working condition of the

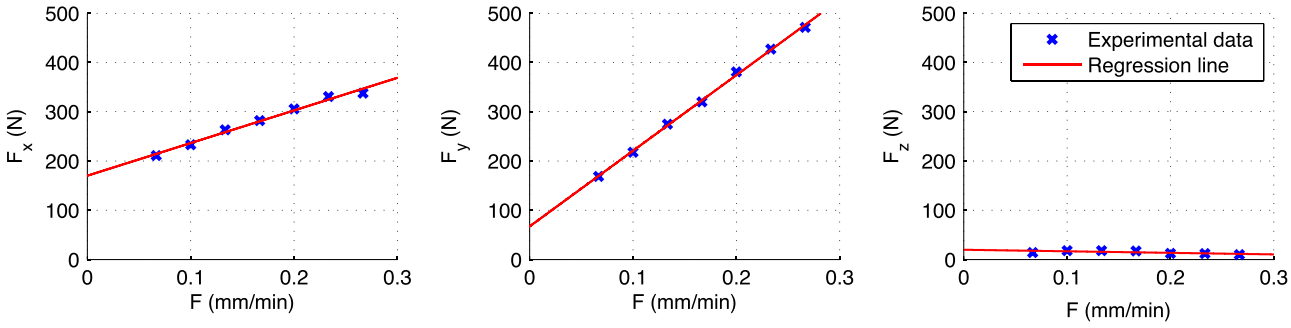


**Fig. 7.** Cutting forces parallel (left) and perpendicular (right) to the feed direction, for different feed rates.

**Table 2**
Cutting force constants for the *AA 6082-T6*.

| Constant | $K_{rc}$ | $K_{re}$ | $K_{tc}$ | $K_{te}$ | $K_{ac}$ | $K_{ae}$ |
|---|---|---|---|---|---|---|
| Value | 264.9 N/mm$^2$ | 53.4 N/mm | 614.1 N/mm$^2$ | 21.1 N/mm | 0 N/mm$^2$ | 3.9 N/mm |

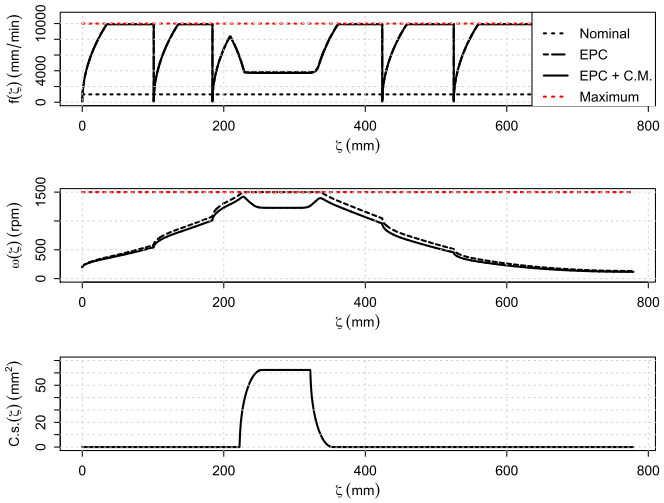


**Fig. 8.** Feed rate (top) and spindle speed (center) utilized for the three cutting tests considered. The cross section (C.S.($\zeta$)) is reported at the bottom.

milling machine is inside of a stability pocket of the stability lobes diagram (Fig. 6).

The surfaces of the cuts obtained in the three tests are shown in Fig. 9. It is possible to observe how the chatter mitigation term of the target function allows the process to remain in a stable condition, without the insurgence of chatter. Indeed, the chatter-free surface appears to be more smooth, and has a lower *Ra* and *Rz* roughness. The roughness of the surfaces was measured through a *Mitutoyo SJ-201P* roughness tester with a tip radius of 2 μm. The base length was set to 2.5 mm, and the number of base lengths was 5.

On the other side, chatter mitigation term (that includes forced vibrations) has a negligible effect on feedrate. As a matter of fact, in machining practice, feedrate increases vibration level (forced) only for hard materials of very demanding cutting parameters. EPC was able almost halve the cutting time, thus enhancing sensibly the process productivity. This was due to the fact that on-air movements were recognized by the EPC and traveled at the maximum allowed feed rate. Moreover the EPC has a richer knowledge of the process and machine utilized, therefore it can execute the cut with a higher feed rate than the one suggested by the tool manufacturer and that represent a compromise value, valid for generic applications.

## 5. Conclusion

An optimal process control – called *Evaluation Perception Controller* (EPC) – for milling process has been developed, aiming at optimizing multi-objective target functions defined in order to reduce production times, costs, and increase the quality of the machined part. The EPC exploits a real-time milling process model and *a priori* knowledge concerned with machine dynamics and phenomena provoking vibrations onset. The effectiveness of the EPC, with particular attention to the stability of the process, was tested by performing cuts on a 3-axes industrial milling machine. The reference process was the full-immersion face milling of a *AA6082-T6* block. The results show how EPC adoption is able to produce a significant increase of the performance in terms of productivity and surface quality; indeed, when the EPC is applied with a target function that considers both productivity and vibrations, the cycle time is reduced by 46% and the surface roughness (*Ra*) by 22%. However, the experimental campaign is

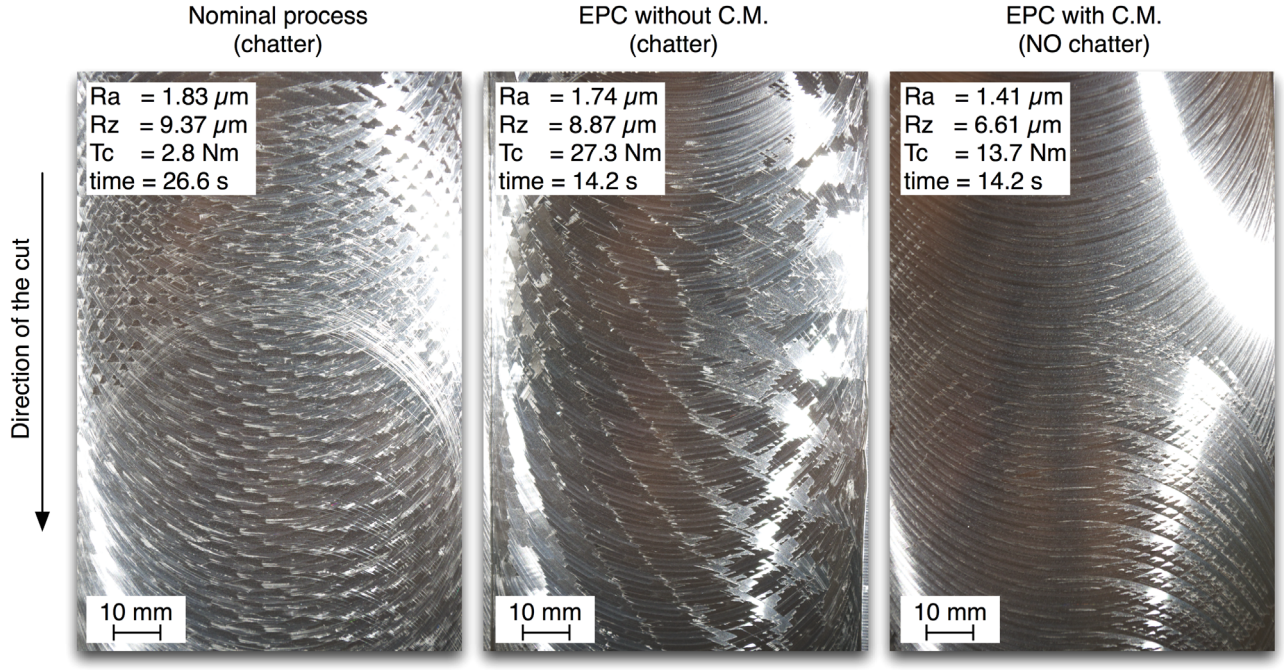


**Fig. 9.** Surfaces and performances obtained for the three considered cuts.

still partial. In particular, future activities will regard:

1. An extended experimental campaign exploring different types of tools, tool paths, machine materials and machine dynamics
2. The development of a methodology to identify the best set of weights of the various components of the multi-objective target function. The weights must be coherent with end-user requirements and might vary along with the milling process under consideration (roughing, semi-finishing, and finishing)
3. The development of "work-around" policies to be activated when the controller is unable to attain the minimum process performance: for instance, when no spindle speed exists able to avoid chatter occurrence

Finally, it is worth to be noted that, thanks to the open nature of the EPC architecture, new performance indicators can be easily introduced and optimized by enriching the multi-objective target function, once a model is available for its real-time estimation (for instance, energy consumption). Therefore, the proposed EPC is candidate for becoming a comprehensive and flexible solution for realizing in practice the paradigm of Intelligent Manufacturing in machine tools sector.

## References


[1] S. Mekid, P. Pruschek, J. Hernandez, Beyond intelligent manufacturing: a new generation of flexible intelligent {NC} machines, Mech. Mach. Theory 44 (2) (2009) 466–476.
[2] W. Brian Rowe, Y. Li, B. Mills, D.R. Allanson, Application of intelligent CNC in grinding, Comput. Ind. 31 (1) (1996) 45–60.
[3] G. Weiss, Multiagent Systems: A Modern Approach to Distributed Artificial Intelligence, Intelligent Robotics and Autonomous Agents Series, MIT Press, Cambridge (US), 1999.
[4] I. Mahdavi, B. Shirazi, A review of simulation-based intelligent decision support system architecture for the adaptive control of flexible manufacturing systems, J. Artif. Intell. 3 (2010) 201–219.
[5] Y. Altinta, E. Budak, Analytical prediction of stability lobes in milling, CIRP Ann. Manuf. Technol. 44 (1) (1995) 357–362.
[6] Y.S. Liao, Y.C. Young, A new on-line spindle speed regulation strategy for chatter control, Int. J. Mach. Tools Manuf. (1996) 651–660.
[7] N.J.M. van Dijk, E.J.J. Doppenberg, R.P.H. Faassen, N. van de Wouw, J.A. J. Oosterling, H. Nijmeijer, Automatic in-process chatter avoidance in the high-speed milling process, J Dyn. Syst. Meas. Control 1322 (March) (2010) 1–14.
[8] Jérémie Monnin, Fredy Kuster, Konrad Wegener, Optimal control for chatter mitigation in milling—Part 1: Modeling and control design, Control Eng. Pract. 24 (May) (2014) 156–166.
[9] M. Pedro, P. Pahud, The Frahm damper, in: Vibration Mechanics, Springer, The Netherlands, 1991, pp. 156–171.
[10] K.J. Liu, K.E. Rouch, Optimal passive vibration control of cutting process stability in milling, J. Mater. Process. Technol. 28 (1–2) (1991) 285–294.
[11] A. Rashid, C.M. Nicolescu, Design and implementation of tuned viscoelastic dampers for vibration control in milling, Int. J. Mach. Tools Manuf. 48 (9) (2008) 1036–1053.
[12] J.L. Dohner, J.P. Lauffer, T.D. Hinnerichs, N. Shankar, M. Regelbrugge, C. M. Kwan, R. Xu, B. Winterbauer, K. Bridger, Mitigation of chatter instabilities in milling by active structural control, J. Sound Vib. 269 (1–2) (2004) 197–211.
[13] E. Abele, H. Hanselka, F. Haase, D. Schlote, A. Schiffler, Development and design of an active work piece holder driven by piezo actuators, Prod. Eng. 2 (4) (2008) 437–442.
[14] H. Moradi, M.R. Movahhedy, G.R. Vossoughi, Robust control strategy for suppression of regenerative chatter in turning, J. Manuf. Process. 11 (2) (2009) 55–65.
[15] H. Moradi, G. Vossoughi, M.R. Movahhedy, H. Salarieh, Suppression of nonlinear regenerative chatter in milling process via robust optimal control, J. Process Control 23 (5) (2013) 631–648.
[16] K.H. Hajikolaei, H. Moradi, G. Vossoughi, M.R. Movahhedy, Spindle speed variation and adaptive force regulation to suppress regenerative chatter in the turning process, J. Manuf. Process. 12 (2) (2010) 106–115.
[17] P. Albertelli, M. Leonesio, G. Bianchi, M. Monno, An analytical approach to optimize sinusoidal spindle speed variation in milling, in: Proceedings of The First International Conference on Process Machine Interactions (CIRP), 2008, Hannover.
[18] J.P. Costes, V. Moreau, Surface roughness prediction in milling based on tool displacements, J. Manuf. Process. 13 (2011) 133–140.
[19] M. Soori, B. Arezoo, M. Habibi, Virtual machining considering dimensional, geometrical and tool deflection errors in three-axis CNC milling machines, J. Manuf. Syst. 33 (4) (2014) 498–507.
[20] M.D. D'Addona, D. Matarazzo, A.M.M.S. Ullah, R. Teti, Tool wear control through cognitive paradigms, Proc. CIRP 33 (2015) 221–226.
[21] B. Li, A review of tool wear estimation using theoretical analysis and numerical simulation technologies, Int. J. Refract. Metals Hard Mater. 35 (2012) 143–151.
[22] S. Doruk Merdol, Yusuf Altintas, Virtual cutting and optimization of three-axis milling processes, Int. J. Mach. Tools Manuf. 48 (August (10)) (2008) 1063–1071.
[23] P. Stavropoulos, D. Chantzis, C. Doukas, A. Papacharalampopoulos, G. Chryssolouris, Monitoring and control of manufacturing processes: a review, Proc. CIRP 8 (0) (2013) 421–425.
[24] A.G. Ulsoy, Y. Koren, Control of machining process, Trans. ASME 115 (1993).
[25] E. Bertolazzi, F. Biral, M. Da Lio, Real-time motion planning for multibody systems, Multibody Syst. Dyn. 17 (2-3) (2007) 119–139.
[26] P. Cannarsa, H. Frankowska, E.M. Marchini, On Bolza optimal control problems with constraints, Discrete Contin. Dyn. Syst. Ser. B 3 (2009) 629–653.
[27] P. Bosetti, M. Leonesio, P. Parenti, On development of an optimal control system for real-time process optimization on milling machine tools, in: Proceedings of The Eighth CIRP Conference on Intelligent Computation in Manufacturing Engineering, 2012, Ischia.
[28] G. Quintana, J. Ciurana, Chatter in machining processes: a review, Int. J. Mach. Tools Manuf. 51 (5) (2011) 363–376.
[29] A. Iglesias, J. Munoa, J. Ciurana, Optimisation of face milling operations with structural chatter using a stability model based process planning methodology, Int. J. Adv. Manuf. Technol (2013) 1–13.
[30] S.S. Park, Y. Altintas, M. Movahhedy, Receptance coupling for end mills, Int. J. Mach. Tools Manuf. 43 (9) (2003) 889–896.
[31] A. Otto, G. Radons, Application of spindle speed variation for chatter suppression in turning, CIRP J. Manuf. Sci. Technol. 6 (2) (2013) 102–109.
[32] M. Born, V. Fock, Beweis des adiabatensatzes, Z. Phys. 51 (3–4) (1928) 165–180.
[33] Y. Altintas, G. Stepan, D. Merdol, Z. Dombovari, Chatter stability of milling in frequency and discrete time domain, CIRP J. Manuf. Sci. Technol. 1 (1) (2008) 35–44.
[34] F.N. Fritsch, R.E. Carlson, Monotone piecewise cubic interpolation, SIAM: SIAM J. Numer. Anal. 17 (1988) 238–246.
[35] D.C. Montgomery, Design and Analysis of Experiments. Student Solutions Manual, John Wiley & Sons, Hoboken, 2008.
[36] Y. Altintas, Manufacturing Automation: Metal Cutting Mechanics Machine Tool Vibrations, and CNC Design, Cambridge University Press, Cambridge (UK), 2000.
[37] I. Bediaga, J. Hernández, J.M. noa, L.L. de Lacalle, An automatic spindle speed selection strategy to obtain stability in high-speed milling, Int. J. Mach. Tools Manuf. 49 (5) (2009) 384–394.
[38] E. Kuljanic, M. Sortino, G. Totis, Multisensor approaches for chatter detection in milling, J. Sound Vib. 312 (4–5) (2008) 672–693.
[39] E. Budak, E.J.A. Armarego, Y. Altintas, Prediction of milling force coefficients from orthogonal cutting data, J. Eng. Ind. 118 (2) (1996) 216–224.